Journal of Sound and Vibration (2002) **253**(4), 917–925
doi:10.1006/jsvi.2001.4057 available online at http://www.idealibrary.com on IDEAL®

MULTI-LAYERED PIEZOELECTRIC INSERTS AS VIBRATION CONTROL ACTUATORS

A. Joshi

Department of Aerospace Engineering, Indian Institute of Technology, Bombay, Powai, Mumbai- 400 076, India. E-mail: ashokj@aero.iitb.ernet.in

(*Received* 19 *January* 2001, *and in final form* 11 *July* 2001)

1. INTRODUCTION

In recent times, developments in smart material technology have led to examination of many new and promising concepts for actuators, using piezoceramic material [1–5]. The most common form of a piezoceramic actuator is either a single thin sheet or a number of discrete rectangular patches, in order to provide sufficient force input. One of the major drawbacks of the single sheet form is the modal phase cancellation which severely restricts the control capability for higher vibration modes of the structure. On the other hand, discrete patches require careful management of higher modes and as a result, the control schemes become highly involved and difficult to implement. A single piezoelectric patch, whether one-sided, or in the bimorph form, has a fairly low voltage-strain sensitivity and hence cannot generate a large control force. In practice, this sensitivity is further eroded due to incomplete strain transfer from structure to the patch, arising out of the characteristics of the bond material. One way of increasing the actuator sensitivity is to use very high input voltages, but this can lead to problems of patch burning as well as additional safety requirements while working with high voltages. Another way is to use a larger number of layers at the same point, one below the other in the thickness direction, which increase the force output for the same input voltage. Further, in many practical applications, it is desired that such patches should be embedded into the surface in order to retain its original shape and these two together have given rise to the concept of multi-layered piezoelectric insert. The present study investigates the non-dimensional voltage-moment sensitivity of such inserts, for various values of patch thickness and modulus ratio, for application as an actuator for vibration control in thin-walled beam-type structures.

2. FREE SURFACE PATCH VERSUS EMBEDDED PATCH

Figure 1(a) shows the schematic of a free surface piezoelectric patch, along with the mechanism of the strain transfer from the parent structure to the patch and it is seen that even though the patch is rigidly attached to the structure, there is a strain diffusion through the thickness of the patch as its top surface does not carry any stress. It is clear from this behaviour that the effective strain experienced by the patch is significantly smaller than the ideal value, assumed in many studies [1–5]. This results in a lower

0022-460X/02/$35.00

sensitivity in the surface-bonded patch, in comparison with the sensitivity achieved in a freely expanding patch.

The concept of embedding the patch in the parent structure alleviates the above problem by providing additional load transfer paths on the side of the patch, as shown in Figure 1(b). It can be seen clearly that when the top surface of the patch is made flush with the top surface of the structure, by making a depression in the structure of the size of the patch, the strain distribution in the patch is identical to the structure, which ensures near-ideal sensitivity of the patch in terms of force generation. Apart from increased sensitivity, an embedded patch offers the advantage of no protruding parts from the surfaces which may have aerodynamic requirements (e.g., wings of aircraft, blades of fans, propellers, turbines, helicopter rotors, etc.). The influence of embedding of the patch in the structure is also favourable from the point of view of overall weight, stiffness and strength of the structure containing the patch, in relation to the surface patch. Thus, embedding the patch in the structure is a better way of using these materials and it also truly justifies the term

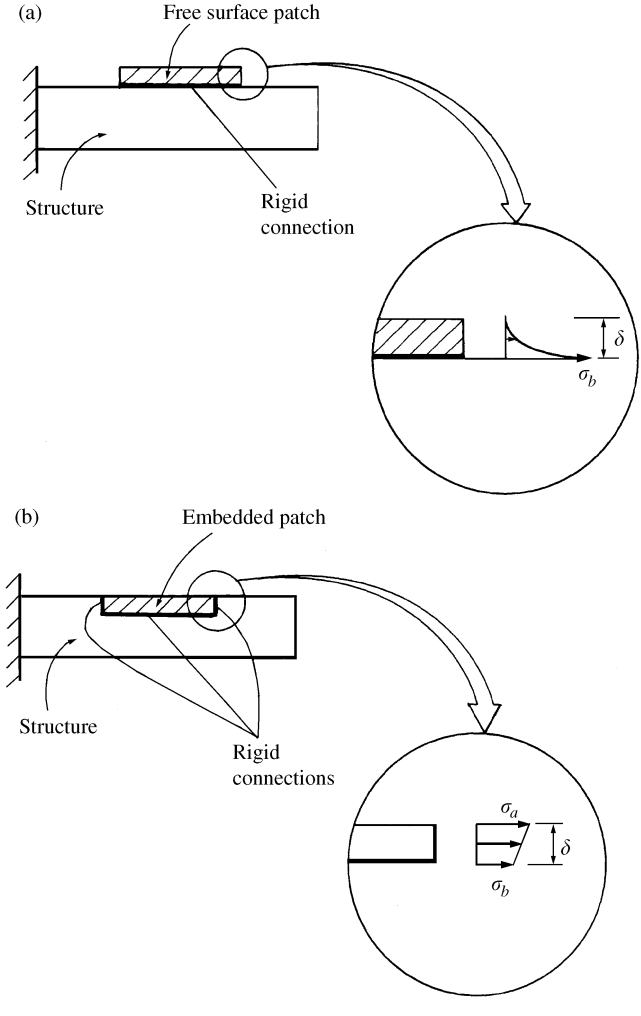

Figure 1. General configuration of free surface piezoelectric patch and stress distribution in a single patch in (a) surface-bonded configuration and (b) embedded configuration.

"smart structure" in such cases, as the control elements become an integral part of the structure itself.

3. CONCEPT OF MULTI-LAYERED PIEZOELECTRIC INSERT

A multi-layered piezoelectric insert can be visualized as a stack which has more than one layer of the patch, in a manner similar to any laminated material. In the present case, each layer is in the standard bimorph configuration (i.e., there is a layer below the neutral axis, corresponding to a layer above the neutral axis) and is required to be electrically insulated from each other. When the above multi-layered configuration is used as an actuator, it is assumed that each layer is supplied with electrical voltage in a manner that produces a pure bending moment in the multi-layered patch. This means that different layers of the patch are required to be energized with voltages which vary linearly with the depth-wise location of each layer. It can be seen that the total moment generated by the patch is an algebraic sum of the moments produced by individual layers, which can be quite large, in comparison with the moment produced by a single-layer patch. It must be mentioned here that the average voltage value over the total patch depth, that is applied to different layers, remains the same as that of the single-layer patch of the same total thickness. In practical applications, an embedded insert needs to follow the external geometry of the surface in which it is to be embedded and in the case of thin-walled beams, an insert of finite width may appear like a cut ring. In the literature, there are no reported studies on the ring-type configuration of the patch, which has the following advantages over a flat patch. Firstly it increases the sensitivity of the patch as it can cover more cross-sectional area in the case of beams with non-rectangular cross-sections. Secondly, it actually provides for a significant cross-axis sensitivity and this property can become quite useful when the direction of external disturbance is either unknown or uncertain. In the present study, the piezoelectric insert is formulated as a ring insert.

4. MULTI-LAYERED INSERT IN THIN-WALLED BEAM-TYPE SHELLS

4.1. RECTANGULAR THIN-WALLED BEAMS

Figure 2(a) shows the cross-sectional geometry of a rectangular thin-walled beam-type shell, carrying a multi-layered piezoelectric patch, all around the cross-section and it is assumed that the insert responds only to deformations normal to its plane. Figure 2(b) shows the strain distribution in the cross-section when a suitable voltage is applied to all the layers of the multi-layered insert. The strain in each layer ε_l and the average strain in the total patch ε_p are given by

$$\varepsilon_l = V_l d_{31}/\delta_l, \qquad \varepsilon_p = V_p d_{31}/\delta_l, \tag{1}$$

while the maximum strain at the beam–patch interface is obtained by imposing the condition of liner strain as

$$\varepsilon_b = [(b-\delta)/(b-\delta/2)]\varepsilon_p, \tag{2}$$

where δ is the total thickness of the multi-layered insert and is given by

$$\delta = \delta_l N. \tag{3}$$

It may be noted here that within each layer of the patch, strain ε_l is different from the average strain ε_p. The total cross-sectional moment developed due to the above average

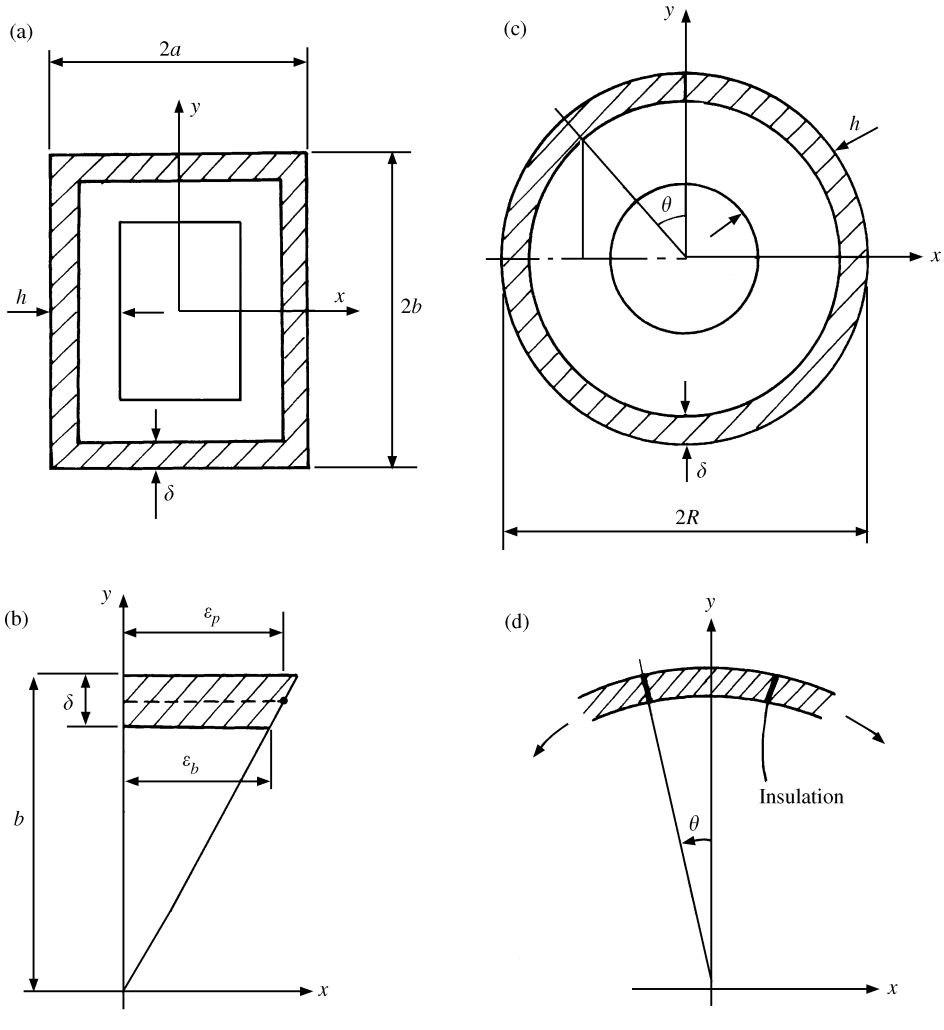

Figure 2. (a) Geometry of a rectangular thin-walled beam with embedded piezoelectric patch. (b) Thickness-wise linearized strain distribution. (c) Geometry of a circular thin-walled beam with embedded piezoelectric patch. (d) Circumferential co-ordinate system.

strain can be expressed as

$$M = M_p + M_b, \tag{4}$$

where M_p is the moment due to the strain in the patch and M_b is the moment due to the strain in the beam and both are given by

$$M_p = 4aE_p\varepsilon_p(b - \delta/2)\delta + (4/3)\delta E_p\varepsilon_p(b - \delta)^3/(b - \delta/2), \tag{5}$$

$$M_b = (4/3)(a - \delta)E_b\varepsilon_p(b - \delta)^3/(b - \delta/2). \tag{6}$$

In the non-dimensional form, the total moment $\bar{M}$, in terms of strain ε_p, is expressed as

$$\bar{M} = [3\bar{\delta}(1 - \bar{\delta}/2)\bar{E}_p + (1 - \bar{\delta})^3/(1 - \bar{\delta}/2)\{(1 - \bar{\delta}\bar{b}) + \bar{\delta}\bar{b}\bar{E}_p\}]\varepsilon_p, \tag{7}$$

where

$$\bar{M} = Mb/(E_b I_0), \quad l_0 = (4/3)ab^3, \quad \bar{b} = b/a, \quad \bar{\delta} = \delta/b. \tag{8}$$

Expression (7) can be rewritten in terms of the non-dimensional average patch voltage $\bar{V}_p$ as

$$\bar{M} = [3\bar{\delta}(1-\bar{\delta}/2)\bar{E}_p + (1-\bar{\delta})^3/(1-\bar{\delta}/2)\{(1-\bar{\delta}\bar{b}) + \bar{\delta}\bar{b}\bar{E}_p\}] \times (\bar{V}_p N/\bar{\delta}), \tag{9}$$

where $\bar{V}_p$ is given by

$$\bar{V}_p = V_p d_{31}/b. \tag{10}$$

The above expression (9) is for a solid rectangular cross-section and the corresponding expression for a thin-walled rectangular section is given as

$$\bar{M}' = [3\bar{\delta}(1-\bar{\delta}/2)\bar{E}_p + (1-\bar{\delta})^3/(1-\bar{\delta}/2)\{(1-\bar{\delta}\bar{b}) + \bar{\delta}\bar{b}\bar{E}_p\}] \times (\bar{V}_p N/\bar{\delta})/\{1-(1-\bar{h}\bar{b})(1-\bar{h})^3\}, \tag{11}$$

where $\bar{M}'$ is given as

$$\bar{M}' = \bar{M}(I_0/I_0'). \tag{12}$$

It may be mentioned here that the expression for the moment sensitivity, given by equation (11), is for the disturbance along y-axis. In case disturbance is either about x-axis or about any other intermediate axis, the above expression needs to be interpreted in an appropriate manner.

4.2. CIRCULAR THIN-WALLED BEAMS

Figure 2(c) shows the cross-sectional geometry of a circular thin-walled beam-type shell, carrying a multi-layered piezoelectric patch, all around the cross-section. It can be seen that due to the curvature of the cross-section, the patch also becomes curved and this fact needs to be incorporated into the sensitivity calculations. Figure 2(d) shows the circumferential direction of the patch, denoted by angle θ, which, in conjunction with Figure 2(b) and equation (1), is used to define the average strain distribution in the total patch, at any circumferential location as

$$\varepsilon_p = \varepsilon_{p0}\cos\theta, \qquad \varepsilon_{p0} = V_{p0} d_{31}\cos\theta/\delta_l, \tag{13}$$

where V_{p0} is the value of the average voltage applied at $\theta = 0$. It can be seen that the voltage distribution is proportional to the distance of the application point from the centre of the circle (from elementary beam theory) and this distance turns out be a cosine function of the circumferential angle θ (see Figure 2(d)). The maximum strain at the beam–patch interface is obtained by imposing the condition of linearity as

$$\varepsilon_{b0} = [(R-\delta)/(R-\delta/2)]\varepsilon_{p0}. \tag{14}$$

The moment components M_b and M_p for a circular beam are given as

$$M_p = \pi E_p \varepsilon_p (R-\delta/2)^2 \delta, \tag{15}$$

$$M_b = (\pi/4)(R-\bar{\delta})^4 E_b/(R-\delta/2)\varepsilon_{p0}. \tag{16}$$

In the non-dimensional form, the total moment $\bar{M}$ can be given as

$$\bar{M} = [4\bar{\delta}\bar{E}_p(1-\bar{\delta}/2)^2 + (1-\bar{\delta})^4/(1-\bar{\delta}/2)]\varepsilon_{p0}, \tag{17}$$

where

$$\bar{M} = MR/(E_b I_0), \qquad l_0 = (\pi/4)R^4, \qquad \bar{\delta} = \delta/R. \tag{18}$$

Expression (17) can be rewritten in terms of the non-dimensional peak value of the average patch voltage $\bar{V}_{p0}$ as

$$\bar{M} = [4\bar{\delta}\bar{E}_p(1-\bar{\delta}/2)^2 + (1-\bar{\delta})^4/(1-\bar{\delta}/2)](\bar{V}_{p0}N/\bar{\delta}), \tag{19}$$

where $\bar{V}_{p0}$ is given by

$$\bar{V}_{p0} = V_{p0}d_{31}/R. \tag{20}$$

The above expression (19) is for a solid circular section and the corresponding expression for a thin-walled circular section is given by

$$\bar{M} = [4\bar{\delta}\bar{E}_p(1-\bar{\delta}/2)^2 + (1-\bar{\delta})^4/(1-\bar{\delta}/2)](\bar{V}_{p0}N/\bar{\delta})/\{1-(1-\bar{h})^4\}. \tag{21}$$

It should be noted that from a practical point of view, the total insert needs to be segmented circumferentially, with an insulating medium in-between, in order to implement a cosine variation of the voltage in the patch. Further, it is to be noted that equation (21) gives the moment sensitivity which is obtained in any cross-sectional direction, for an insert covering complete circumference.

5. ACTUATOR SENSITIVITY RESULTS OF MULTI-LAYERED INSERT

5.1. ADVANTAGES OF MULTI-LAYERED ACTUATOR CONFIGURATION

It is seen from the relation given by equation (1) that for a given voltage, the strain developed in the patch is inversely proportional to the patch thickness and thus a thinner patch is a better actuator. However, strain produced by a single thinner patch acts over a smaller sectional area and thereby generates a smaller bending moment only. In addition, its structural strength is much lower so that it cannot really sustain very large strains produced by applying larger voltages, leading to breakage.

Therefore, it makes greater sense to use smaller voltages on thinner patches which result in higher electric fields and, thereby, same moments as those produced by thicker patches subjected to larger voltages. Further, by using a large number of thinner patches in a parallel configuration, the resulting moment can be multiplied manifolds. Thus, a multi-layered insert helps in significantly reducing the excitation voltages and eliminates the need to have high-voltage amplifiers. In addition, multi-layered patch configuration increases the cross-sectional area of the patch material in the thickness-wise direction, which contributes to much higher sensitivity even for thicker individual patches. finally, actuator sensitivity is directly proportional to the piezoceramic constant d_{31}, which should be large enough and therefore PZT (lead zirconate titanate) is an ideal actuator material possessing a fairly high d_{31}.

5.2. ACTUATOR SENSITIVITY FOR RECTANGULAR THIN-WALLED BEAM

It is seen from equation (11) that for a given total patch thickness, the moment varies linearly with number layers and this indicates that as the number of layers are increased, the thickness of individual layers would reduce. Figure 3(a) shows the variation of a normalized moment parameter $(\bar{M}/\bar{V}_p N)$ as a function of the total patch thickness parameter $\bar{\delta}$, for different values of the modulus parameter $\bar{E}_p$, for a solid square beam (i.e., $\bar{b} = 1$). The range of patch thickness parameter $\bar{\delta}$ is arrived at, considering a single

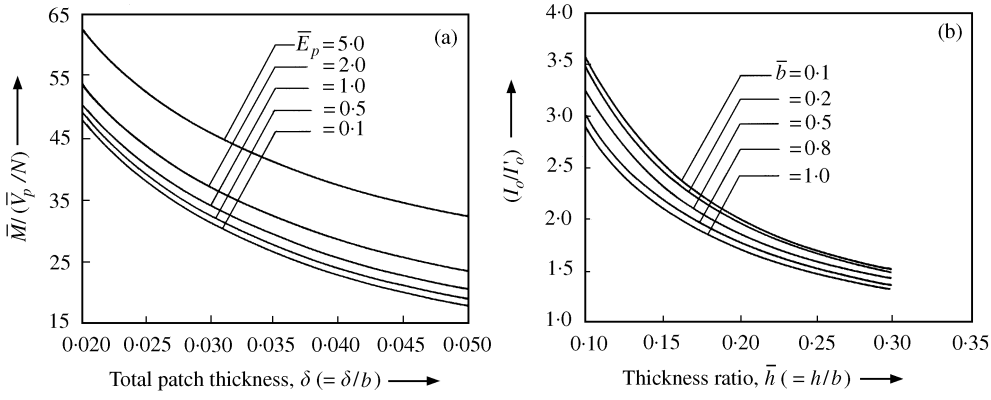

Figure 3. (a) Variation of non-dimensional moment-voltage sensitivity of rectangular beam as a function of the normalized total patch thickness. (b) Variation of the normalized sectional inertia of the thin-walled rectangular beam.

patch to be nominally about 50–100 μm thick and the range for the modulus parameter $\bar{E}_p$ is arrived at by assuming the patch modulus to be nominally about 4.0×10^{10} [6]. It is seen from Figure 3(a) that normalized moment sensitivity varies hyperbolically with total patch thickness parameter $\bar{\delta}$, confirming the fact that a smaller thickness leads to higher sensitivity.

The same increase can also be achieved if there is more than one layer of the patch which is thinner, though the total thickness of the patch may not be very small. Lastly, the sensitivity curve also shows that higher moment can be obtained for a lower input voltage if larger number of patch layers are used. The effect of modulus parameter is such that a patch, with modulus higher than the parent structure, provides a larger moment for the same thickness or provides the same moment at much higher total patch thickness. It is also seen from equation (11) that $\bar{M}$ is a function of $\bar{b}$, for values of $\bar{E}_p \neq 1$. This effect arises due to the web part of the piezoelectric ring insert and its effect is such that for higher $\bar{E}_p$, $\bar{M}$ is higher and for lower $\bar{E}_p$, $\bar{M}$ is lower, in relation to the values obtained for $\bar{E}_p = 1$. Further, this influence is also a function of the sectional height parameter $\bar{b}$. Figure 3(b) presents the variation of the sectional moment of inertia ratio (I_0/I_0') for the rectangular beam, as a function of the sectional thickness ratio $\bar{h}$ and it is seen that (I_0/I_0') increases hyperbolically as thin-walled sections become thinner. It is worth mentioning here that the results for moment sensitivity in respect of thin-walled beams of various thicknesses can be obtained by simply multiplying the results presented in Figures 3(a) and 3(b).

5.3. ACTUATOR SENSITIVITY FOR CIRCULAR THIN-WALLED BEAM

Figure 4(a) shows the variation of moment sensitivity parameter $(\bar{M}/\bar{V}_p N)$ as a function of total patch thickness parameter $\bar{\delta}$, for different values of the modulus parameter $\bar{E}_p$, for a circular beam and it is seen that trends are similar to the ones observed in Figure 3(a) for a square beam. The normalized moment sensitivity in the case of circular beams is only marginally lower, bringing out near invariance of $(\bar{M}/\bar{V}_p N)$ to sectional geometry. This is an important observation which indicates that the results obtained in respect of the moment sensitivity parameter $(\bar{M}/\bar{V}_p N)$ for either rectangular of circular beams can be directly applied to a wide range of cross-sectional geometries, which are not regular in nature so that such an analysis would be difficult to perform.

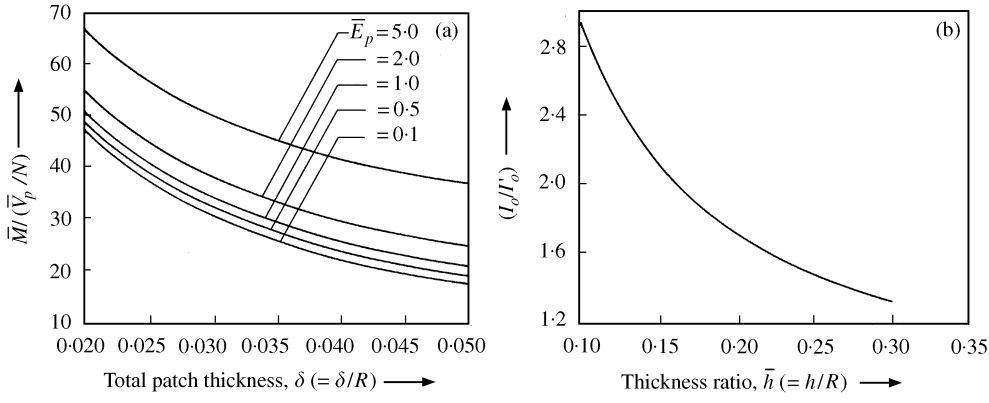

Figure 4. (a) Variation of non-dimensional moment-voltage sensitivity of circular beam as a function of the normalized total patch thickness. (b) Variation of the normalized sectional inertia of the thin-walled circular beam.

6. CONCLUSIONS

The present study has developed the conceptual model of a multi-layered piezoelectric ring insert as vibration control actuator. The multi-layered patch is postulated as a combination of a large number of thinner bimorph patch pairs, which are stacked over each other in the manner of a laminated composite material, and are electrically insulated from each other. The concept of embedding the patch into the surface makes its application convenient for aerodynamic surfaces as well as results in minimal changes to the mass, stiffness and strength properties of the structure as a whole. Next, the moment sensitivity of the multi-layered patch is investigated, using the elementary beam theory and results are obtained for two typical thin-walled beam cross-sections. The patch is postulated in the form of a ring, by virtue of its embedding into the surface and having finite width, which also gives rise to the cross-axis sensitivity as an additional benefit. The non-dimensional expressions are obtained in terms of the total patch thickness parameter, patch modulus parameter and applicable geometrical parameters of the cross-section. These results show that it is possible to generate large control moments, by applying much smaller voltages, using a large number of thinner patches. Finally, the results obtained here are considered to be applicable to many other non-regular cross-sectional geometries, which are difficult to model analytically.

ACKNOWLEDGMENTS

The work reported in this paper forms a part of the project sponsored by the Extra Mural Research (EMR) Division of the Council of Scientific and Industrial Research (CSIR), New Delhi, India. The financial support received is gratefully acknowledged.

REFERENCES

1. E. H. Anderson and N. W. Hagood 1992 *AIAA/ASME/ASCE/AHS/ASE* 33*rd Structures, Structural Dynamics and Materials Conference*, Vol. 2, 2141–2156. Self sensing piezoelectric actuation: analysis and application to controlled structures.

2. R. Berret 1994 *American Institute of Aeronautics and Astronautics Journal* **21**, 1689–1699. Intelligent structures for aerospace: a technology overview and assessment.
3. H. Janocha, D. J. Jendritza and P. Scheer 1996 *SPIE Conference Proceedings*, Vol. **2779**, 603–609. Smart actuators with piezoelectric materials.
4. T. Takigami, K. Oshima and Y. Hayakawa 1997 *Proceedings of the Americal Control Conference*, Vol. 3, 1867–1872. Application of self-sensing actuator to control of a cantilever beam.
5. J. N. Reddy 1999 *Engineering Structures* **21**, 568–593. On laminated composite plates with integrated sensors and actuators.
6. *Piezoelectric Motor/Actuator Kit Manual*. Peizo Systems Inc. 186, Massachuesetts Avenue, Cambridge, MA, U.S.A.

APPENDIX A: NOMENCLATURE

a	semi-width of rectangular section without patch
b	semi-depth of rectangular section without patch
$\bar{b}(= b/a)$	cross-sectional depth ratio of rectangular section
d_{31}	strain-voltage sensitivity constant of piezoelectric material
E_b	Young's modulus of the beam material
E_p	Young's modulus of the patch material
$\bar{E}_p\ (= E_p/E_b)$	non-dimensional patch modulus parameter
h	wall thickness of the thin-walled beam
$\bar{h}\ (= h/b;\ h/R)$	non-dimensional wall thickness ratio
I_0, I_0'	sectional inertia without patch (solid, thin-walled)
M, M_b, M_p	bending moment, beam contribution, patch contribution
$\bar{M}\ (= Mb(R)/\{(E_b I_0)$	non-dimensional bending moment parameter
N	number of piezoelectric patch layers
R	outer radius of the circular beam without patch
V_l	voltage applied to a single layer
V_p	average voltage applied to the total patch
V_{p0}	average voltage applied to the total patch at $\theta = 0$
$\bar{V}_p(= V_p d_{31}/b(R)\delta)$	non-dimensional value of the average patch voltage V_p
x, y	sectional co-ordinate system
δ	total thickness of the multi-layered patch
δ_l	thickness of a single layer
ε_b	longitudinal strain at the patch–beam interface
ε_{b0}	value of ε_b at $\theta = 0$
ε_l	longitudinal strain in a single-patch layer
ε_p	longitudinal average strain in the total patch
θ	angular co-ordinate of circular beam